Separation Science and Technology
Publication details, including instructions for authors and subscription information:
http://www.informaworld.com/smpp/title~content=t713708471

Preliminary Results for the Investigation of Hydrodynamic Scaling Relationships in Shallow Spouted Beds

Irma D. Lima Rojas[a]
[a] Department of Chemical and Biomolecular Engineering, University of Tennessee, Knoxville, TN, USA

Online publication date: 30 August 2010

To cite this Article Lima Rojas, Irma D.(2010) 'Preliminary Results for the Investigation of Hydrodynamic Scaling Relationships in Shallow Spouted Beds', Separation Science and Technology, 45: 12, 1928 — 1934
To link to this Article: DOI: 10.1080/01496395.2010.494711
URL: http://dx.doi.org/10.1080/01496395.2010.494711

Separation Science and Technology, 45: 1928–1934, 2010

ISSN: 0149-6395 print/1520-5754 online
DOI: 10.1080/01496395.2010.494711

Taylor & Francis
Taylor & Francis Group

Preliminary Results for the Investigation of Hydrodynamic Scaling Relationships in Shallow Spouted Beds

Irma D. Lima Rojas
Department of Chemical and Biomolecular Engineering, University of Tennessee, Knoxville, TN, USA

This research is targeted at developing improved experimentally based scaling relationships for the hydrodynamics of shallow, gas-spouted beds of dense particles. The work is motivated by the need to more effectively scale up shallow spouted beds used in processes such as in the coating of nuclear fuel particles where precise control of solids and gas circulation is critically important. Experimental results reported here are for a 50 mm diameter spouted bed containing two different types of bed solids (alumina and zirconia) at different static bed depths and fluidized by air and helium. Measurements of multiple local average pressures, inlet gas pressure fluctuations, and spout height were used to characterize the bed hydrodynamics for each operating condition. Follow-on studies are planned that include additional variations in bed size, particle properties, and fluidizing gas. The ultimate objective is to identify the most important non-dimensional hydrodynamic scaling groups and possible spouted-bed design correlations based on these groups.

Keywords fluidized beds; hydrodynamic relationships; scaling groups; scaling spouted beds; shallow spouted beds

INTRODUCTION

Spouted beds are widely used for gas-solids contacting where high solids circulation is important. Typically, spouted beds have a central gas jet that entrains solids near the bottom of the bed and transports them upward through a central zone toward the top. As the upward-moving solid particles exit the top of the bed and separate from the gas, they fall back to the bed surface and move slowly downward in an outer annular zone toward the bottom (1). The net effect of these two opposing solids flows is to create a toroidal-like circulation cell that defines the overall solids circulation. The interface between the upward and downward moving solids is not rigid but can vary in space and time. In some cases a cylindrical draft tube is inserted in the center of the bed to stabilize the interface (2,3). This enhances the separation between the upward and downward flow zones and increases the overall circulation rate.

Industrial applications of spouted beds include combustion, coating, drying, and gasification (4–6). There are at least four widely used spouted-bed configurations: flat-base cylindrical, conical-base cylindrical, conical, and dilute jet. Bi (7) reviews many of the salient differences among these designs. In the majority of applications in conical-base beds, the solids bed height in the cylindrical section is deeper than the height of the conical bottom (8); this is termed a "deep bed."

For many types of unit operations, proper scaling is critical in relating laboratory studies to full-scale production. This is also true for spouted beds, where it is desirable to conduct laboratory studies at ambient conditions that can still be relevant to commercial units operating at elevated pressure and temperature. However, scaling up a process involves more than the useful laboratory studies; it requires that some parameters for the larger beds preserve the same values of the small one, which in turn provokes uncertainty on scale-up criteria. The basic groundwork for scaling in fluidized beds in general (which includes spouted beds as a subset) has been discussed in numerous previous studies, most notably in the pioneering work of Glicksman (9,10). However, scaling of spouted beds still remains a relatively undeveloped area.

To address scaling, it is first necessary to identify the key non-dimensional groups that control the hydrodynamics. In the approach of Glicksman (11,12), Horio (13) and others, the principal dimensionless groups underlying the fluidized-bed hydrodynamics are identified by non-dimensionalizing the appropriate momentum and mass conservation equations for the gas and solids. As a result of his analysis, Glicksman et al. (11) determined that the appropriate dimensionless groups defining the hydrodynamics of fluidized beds are $\frac{gd_p}{U^2}, \frac{\rho_s d_p U}{\mu_g}, \frac{\rho_g}{\rho_s}, \frac{H_0}{d_p}, \frac{D_c}{d_p}, \frac{L_1}{L_2}$, $DPSD$, ϕ_s, where g is the gravitational acceleration, d_p is the particle diameter, U is the superficial gas velocity, ρ_s is the solids density, ρ_g is the gas density, H_0 is the static bed depth, D_c is the bed cylinder diameter, L_1 and L_2

Received 26 October 2009; accepted 8 May 2010.
Address correspondence to Irma D. Lima Rojas, Department of Chemical and Biomolecular Engineering, University of Tennessee, 1618 Chenoweth Circle, Knoxville, TN 37909, USA. Tel.: 865-558-0707. E-mail: ilimaroj@utk.edu

are characteristic lengthscales, DPSD is the dimensionless particle size distribution, and ϕ_s is the solids sphericity.

In more recent work, He et al. (14), from considering mechanical effects in the annulus zone, proposed two additional dimensionless numbers: the internal friction angle, ϕ, and the loose-packed voidage, ε_o. They experimentally validated their predictions on the basis of measurements of maximum spoutable bed depth, spout diameter, fountain height, and pressure profiles in the annulus as functions of static bed height.

Still more recently, Xu et al. (15) added the particle-particle coefficient of restitution (e_{ss}) to the scaling relationships of spouted beds proposed by He et al. (14) This parameter was included based on their analysis of the kinetic energy of colliding particles in the spout and annulus regions. Their conclusions seem to be supported by Goldschmidt et al. (16), who also claimed that the flow dynamics of gas-solids systems, such as the bed expansion ratio, are sensitive to e_{ss}. Xu et al. (15) experimentally validated their predictions on the basis of measurements of fountain height, spout diameter, and voidage profiles with changing coefficients of restitution.

Considering the above, the complete list of key dimensionless groups to consider in spouted bed scaling should include: $\frac{gd_p}{U^2}, \frac{\rho_s d_p U}{\mu_g}, \frac{\rho_g}{\rho_s}, \frac{H_0}{d_p}, \frac{D_c}{d_p}, \frac{L_1}{L_2}, DPSD, \phi_s, \varphi, \varepsilon_o, e_{ss},$ This list of dimensionless groups is by no means exhaustive. One would also expect that geometric ratios associated with bed shape and configuration would be important for scaling, as they are needed to define the boundary conditions for the continuity and momentum equations. Finally, it should be noted that the combination of the size distribution and shape of actual particles cannot be captured in the single-value descriptors used in these dimensionless groups. As yet, rigorous ways to include this variability aspect in dimensionless terms have not been defined.

Given the above key scaling groups, it should be theoretically possible to accurately scale from any spouted bed to any other, as long as the same values are maintained for each of the groups. In practice however, it is virtually impossible to match all of the groups simultaneously on two different beds, thus one is typically constrained to focus on recognizing the most important groups in a particular context and matching those as much as possible. Such reduced-order scaling can still be effective as long as the local hydrodynamic features are dominated by the accessible subset of dimensionless groups. The difficulty of experimentally controlling all of the dimensionless groups simultaneously is also why only a subset of the above dimensionless groups (or a rearrangement of a subset) is typically included in experimentally derived correlations (17–22). Once the range of conditions utilized to derive correlations is exceeded (i.e., one uses them to extrapolate), the potential accuracy of predictions can be decreased considerably. Such losses of accuracy should not be surprising since the relative importance of the missing dimensionless groups can increase considerably outside the experimental limits. Furthermore, the fact that scaling fluidized or spouted beds commonly require some fixed parameters such as materials nature and shape justifies the lack of some unimportant dimensionless groups on the scaling and hydrodynamic predictions.

As noted previously, the correlations in the spouted-bed literature are dominated by deep beds of particles with densities of less than $3000\,kg/m^3$. The only correlations relevant to the shallow, dense category are those developed by Zhou (24), who focused his study on defining the hydrodynamics of shallow beds similar to those beds used to coat TRISO fuel particles but at ambient temperature, using ZrO_2 (yttrium-stabilized zirconia, or YSZ, with a material density of $6100\,kg/m^3$) as surrogate fuel particles. Zhou determined the effect of the cone angle, static height, and particle size over the minimum spouting velocity, overall pressure drop and fountain height. Thus the focus of this study will be on expanding the earlier work of Zhou to include more of the key dimensionless groups and increase the range for accurate scaling predictions, especially scaling predictions involving changes in bed size, inlet diameter, particle density, gas viscosity, and gas density. Bed size and gas properties are included because they directly relate to scaling from small, ambient laboratory experiments to hot, production-scale beds.

EXPERIMENTAL

Apparatus

A schematic of the experimental setup is shown in Fig. 1. The spouted bed used in these experiments was fabricated from a 150 mm long quartz tube fitted at the bottom with a 60° included angle aluminum cone. The bottom cone had a height equal to the diameter of the cylinder. A leveler located right below the cone was used to insure fully vertical

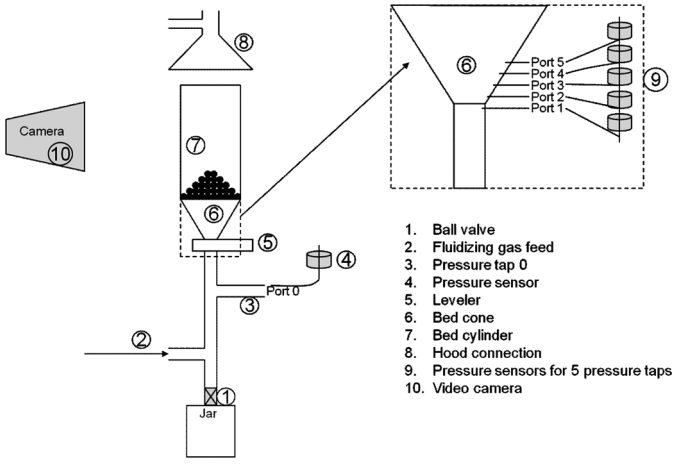

FIG. 1. Schematic of the experimental apparatus.

orientation. At the end of each experiment, the solid particles were drained to a collector jar via a discharge valve.

The 50 mm spouted bed has 6 pressure taps. The first pressure tap, designated as Port 0 and located approximately 10 diameters of the cone inlet upstream from the base of the aluminum cone, was used to measure average and dynamical global pressure drops. From the average global pressure the minimum spouting velocity (U_{ms}) was determined by monitoring the global pressure drop as gas flow was reduced from a fully spouting condition to a nearly packed bed. The minimum spouting velocity was defined as the flow where the pressure drop abruptly increased (see Fig. 2).

Of the remaining five pressure taps (local pressure drops), four were located on the side of the cone at 2, 4, 8, and 16 mm measured from the base of the cone, and one 2 mm below the base of the cone. All six taps were connected to pressure transducers. Depending on the dynamic pressure range, taps were connected to either single-sided Endevco 8510B-1 transducers or to MKS Baratron 223B-type differential pressure transducers with different full-scale ranges.

Gas flow was controlled using 1559A, 1579A, and 1179A MKS mass flow controllers and was humidified to approximately 40% relative humidity in a countercurrent humidification chamber to minimize static charge buildup. The experimental particles were 500 and 1000 μm diameter sizes of alumina (4000 kg/m^3) and yttrium-stabilized zirconia (6100 kg/m^3). Static bed heights were 42% and 67% of the cylinder diameter, respectively, and gas flow rates ranged from about 1.2 to 2.1 U/U_{ms}. Particle densities were determined from the water displacement method. Helium and air fluidizing gases are used to simulate the effect of temperature on the bed hydrodynamic behavior. The effect of the *DPSD*, ϕ_s, ε_0, and e_{ss} on the hydrodynamics behavior is not considered in this study, as particle properties, in a practical sense, are not expected to change with the reactor size.

At each selected operating condition, the mean and transient pressures at each of the six wall pressure taps

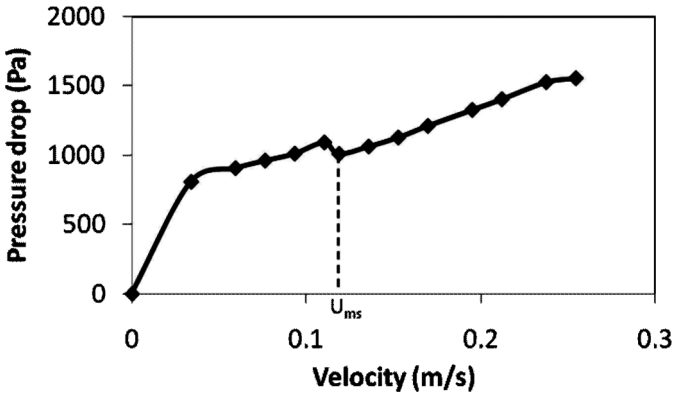

FIG. 2. Determination of U_{ms} on the 50 mm bed for 75 g of 500 μm of ZrO_2 particles.

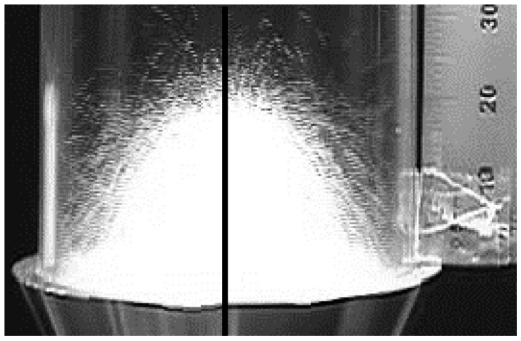

FIG. 3. Composite image at 1.65 U/U_{ms}, with 0.67 H_0/D_c of 500 μm ZrO_2 particles.

and the time-averaged fountain height were measured to characterize the hydrodynamic state. All six pressure signals were recorded at a sampling rate of 1000 Hz for duration of one minute. From the unfiltered transient pressure signals the mean pressure drops at different locations were determined by averaging. The dynamic pressure signals were also low-pass filtered at 100 Hz and then characterized in terms of their frequency content and time-series statistics for diagnostics purposes. A consumer-grade video camera (Sony) was used to record the fountain fluctuations at 30 frames per second for segments of over one minute at each condition, simultaneously with the pressure measurements. The average fountain height is obtained by creating a composite image (see Fig. 3) from a set of 30 randomly selected frames from one-minute video recordings and then using image analysis to determine the mean fountain height as illustrated in Fig. 4.

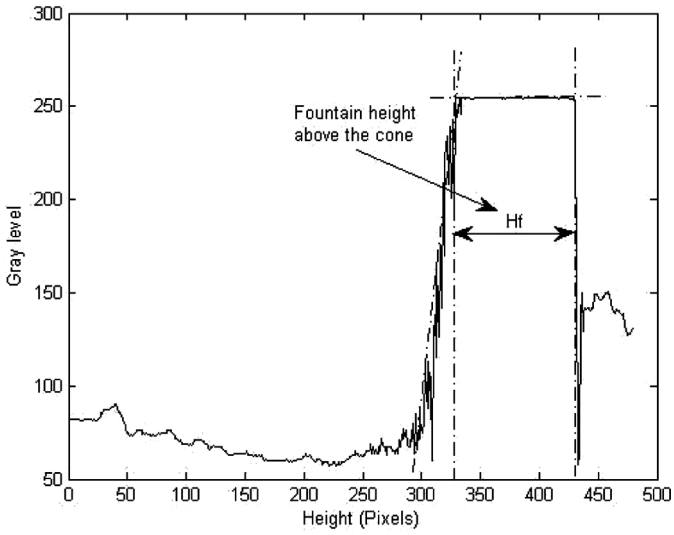

FIG. 4. Diagram illustrating the procedure for fountain height (H_f) measurement at 1.65 U/U_{ms}, with 0.67 H_0/D_c of 500 μm ZrO_2 particles. The vertical axis indicates the gray-scale intensity determined from a pixel-by-pixel analysis along the centerline of the composite digital image.

RESULTS AND DISCUSSION

Minimum Spouting Velocity

Table 1 includes a list of the minimum spouting velocity (U_{ms}) and overall pressure drop (ΔP) obtained for different combinations of the operating parameters in the 50 mm bed. It can be observed that U_{ms} increases with increasing static bed height, particle diameter and particle density, and decreasing fluidizing gas density. Based on these experimental observations, an analysis of variance revealed that the most significant dimensionless factors for defining U_{ms} are $H_0/D_c, d_p/D_c$, Ar and Re_{ms}, where Ar is the Archimedes number and Re_{ms} is the Reynolds number at minimum-spouting conditions.

A regression analysis based on the results depicted in Table 1 suggested the following type of correlation:

$$Re_{ms} = 0.5\left(\frac{H_0}{D_c}\right)^{1.166}\left(\frac{d_p}{D_c}\right)^{0.79} Ar^{0.59} \qquad (1)$$

Figure 5 compares the predictions of this correlation with the experimental U_{ms} values. The regression coefficient is 0.98.

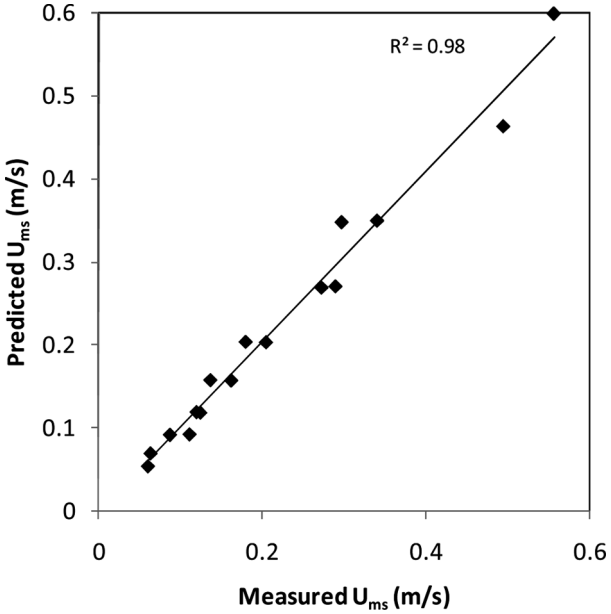

FIG. 5. Predicted U_{ms} vs. measured U_{ms}.

Pressure Drop

The focus of this discussion is on the time-average pressure drop measured from the lowest pressure tap (Port 0). Figure 6 illustrates an interesting difference in the spouted-bed behavior with air versus helium fluidization. With air, the pressure drop across the bed was nearly constant while fluidizing particles up to $U/U_{ms} = 2$. However for helium, the pressure is not constant after $U/U_{ms} = 1.8$ but begins to rise slowly with flow. Visually, the spouting regime with helium also appeared to be highly unstable and unsteady at the higher flow rates, resulting in a higher pressure-signal variance. Also, it can be observed that the pressure drop across the bed for helium as fluidizing gas is larger than for air. All of the above changes reflect important changes in the spouting hydrodynamics related to the lower gas viscosity and density of helium relative to air.

At very low gas flows there were also important differences between air and helium fluidization. The different gas properties appeared to affect the packing and flow behavior of the particles at near the gas inlet. With air, the pressure drop reached a maximum value, and then started to rapidly decrease until the particles began to fall into the gas inlet tube. With helium, the particles began to collect more smoothly near the inlet tube at higher flows.

Preliminary data analysis revealed that the most significant dimensionless factor for correlating the pressure drop at minimum spouting (ΔP_s) is the Archimedes number (Ar). From the data listed in Table 1, two correlations were fit by

TABLE 1
U_{ms} values at different particle size, particle density, static height and gas density for the 50 mm spouted bed

Particle material	Particle size (μm)	H_0/D_c	Air		Helium		Air-Helium difference	
			U_{ms} (m/s)	ΔP (Pa)	U_{ms} (m/s)	ΔP (Pa)	U_{ms} (%)	ΔP (%)
Al_2O_3	500	0.42	0.06	408.0	0.09	453.3	45.4	11.1
Al_2O_3	500	0.75	0.11	604.2	0.14	690.4	23.0	14.3
Al_2O_3	1000	0.42	0.16	340.0	0.27	395.4	68.3	16.3
Al_2O_3	1000	0.67	0.29	486.8	0.49	576.1	71.1	18.4
ZrO_2	500	0.42	0.06	590.4	0.12	665.6	96.5	12.8
ZrO_2	500	0.67	0.12	880.7	0.18	1033.8	50.6	17.4
ZrO_2	1000	0.42	0.20	498.9	0.30	581.9	45.4	16.7
ZrO_2	1000	0.67	0.34	759.1	0.56	898.0	63.6	18.3

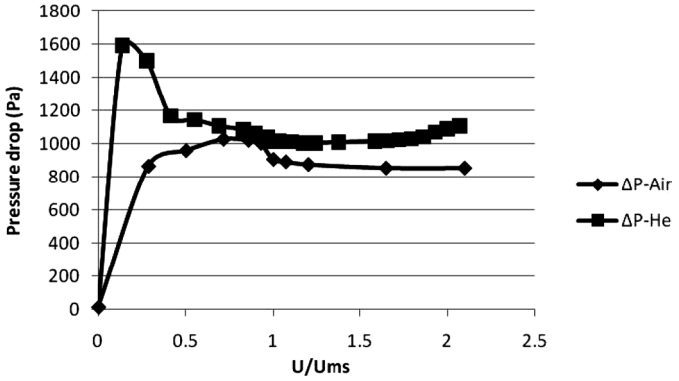

FIG. 6. Average pressure drop at Port 0 of the 50 mm diameter spouted bed as a function of U/U_{ms} for $H_0/D_c = 0.67$ of 500 μm ZrO_2 particles with air and helium as fluidizing gases.

regression; the coefficients of regression are 0.92 and 0.97 for Eqs. (2) and (3) respectively (see Fig. 7).

$$\frac{\Delta P_s}{\rho_s H_0 g} = 1.087(Ar)^{-0.081} \tag{2}$$

Another form of ΔP_s in terms of Re_{ms} is given by Eq. (3)

$$\frac{\Delta P_s}{\rho_s H_0 g} = 1.01(\mathrm{Re}_{ms})^{-0.132}\left(\frac{H_0}{D_c}\right)^{0.022}\left(\frac{d_p}{D_c}\right)^{0.1} \tag{3}$$

Fountain Height

At gas flows below 2.1 U/U_{ms}, the time-average fountain height appears to vary linearly with gas flow for all cases listed in Table 1 (see Figs. 8 and 9), beyond which

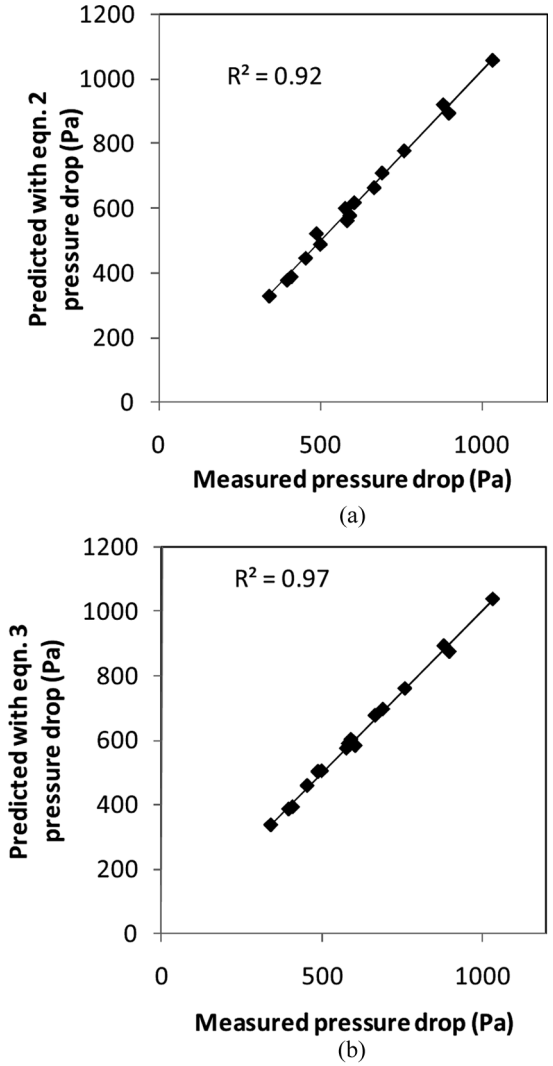

FIG. 7. Predicted ΔP vs. measured ΔP.

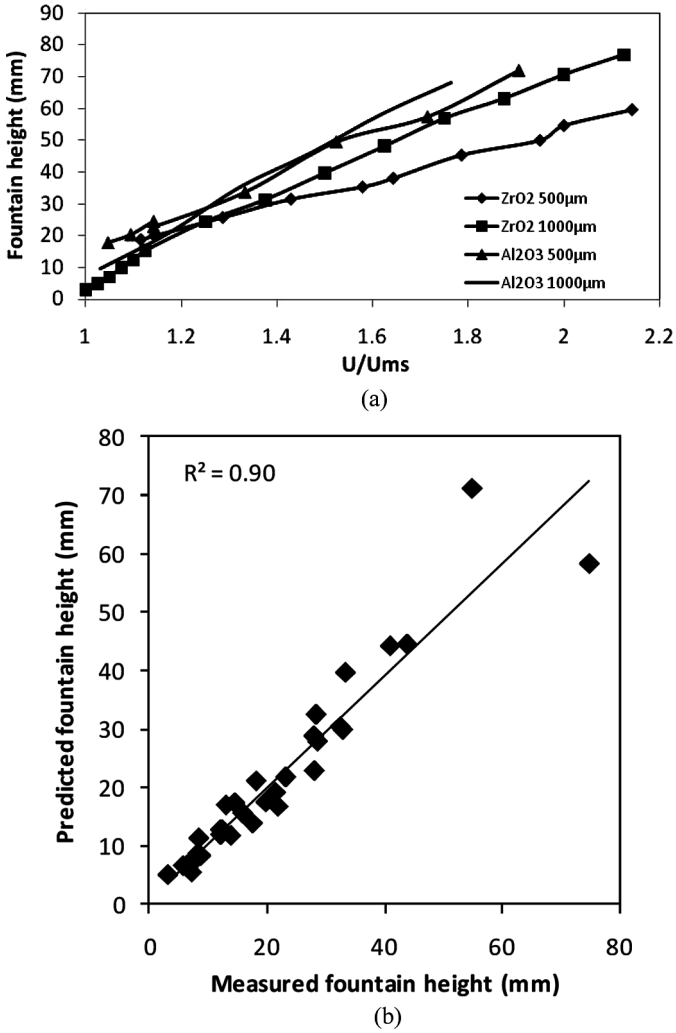

FIG. 8. (a) Effect of gas flow rate on fountain height of 50 mm diameter spouted bed for different sizes of ZrO_2 and Al_2O_3 at 0.75 H_0/D_c; (b) Predicted H_f vs. measured H_f.

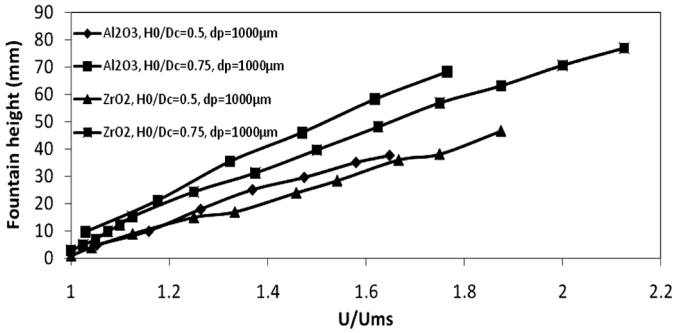

FIG. 9. Fountain height as a function of U/U_{ms} measured on the 50 mm diameter spouted bed with $H_0/D_c = 0.75$ and 0.5 with 1000 μm ZrO_2 and Al_2O_3 particles.

the estimate of time-average fountain height is less certain due to larger fluctuations of the fountain height. Also noteworthy is how the linear trends for 500 and 1000 μm particle diameters overlap between 1.2 and 1.6 U/U_{ms} for Al_2O_3; for ZrO_2, the linear trends overlap just between 1.2 and 1.4 U/U_{ms}. On the other hand, it can be seen that the static bed height, particle density, and the gas flow rate are the most important interacting factors that have a major effect on the fountain height.

The most significant dimensionless factor for correlating the fountain height are $\frac{H_f}{H_0}, \frac{U}{U_{ms}}, \frac{H_0}{D_c}, \frac{d_p}{D_c}$, Ar and Re_{ms}. From the measurements of fountain height done to the listed cases in Table 1 at 1.65 U/U_{ms} and 1.2 U/U_{ms}, a correlation was fit by regression with a coefficient of regression of 0.9 (see Fig. 8).

$$\frac{H_f}{H_0} = 0.33\left(\frac{U}{U_{ms}}\right)^{2.95}\left(\frac{d_p}{D_c}\right)^{-2.96}\left(\frac{H_0}{D_c}\right)^{-4.05}(Ar)^{-1.95}(Re)^{3.57} \quad (4)$$

CONCLUSIONS

Minimum spouting velocity for a fixed, shallow spouted bed operating with dense particles was found to increase with increasing static bed height, particle diameter and particle density, and also with decreasing fluidizing gas density. A preliminary analysis indicates that all of these effects can be correlated with a simple function relating the particle Reynolds number at minimum spouting condition to dimensionless forms of the particle diameter and bed height and the Archimedes number. This seems to be generally consistent with the results of Mathur and Gishler (18), although not all of the parameters they considered were included in this preliminary study. This study extends this trend to shallower beds and denser particles than have been previously reported.

It was found that the overall pressure drop increases with increasing static bed height and particle density and with decreasing particle diameter and fluidizing gas density. According to other authors such as Mukhlenov and Gorshtein (23) and Olazar et al. (20), the pressure drop decreases as Re_{ms} increases, and increases as H_0 and Ar increase. Simple functional forms relating the dimensionless pressure drop to the Archimedes number or the minimum spouting particle Reynolds number and dimensionless particle diameter and static bed height were found to give good fits to the present experimental data.

The trends of fountain height observed here were more complex that the trends in minimum spouting velocity and pressure drop. Other studies such as those by Grace and Mathur (25), Day (26), San José et al. (27), and Zhou (24) found that the larger the cone inlet diameter, U/U_{ms}, and ε_0, the larger the H_f; also, the larger ρ_s, the smaller H_f. However, the effect of static bed height appear to be contradictory. The result obtained in this study specifies that H_f increases with increasing gas flow rate, gas density, particle diameter, and static bed height and decreasing particle density. The effect of the temperature on the fluidization gas is simulated using different gases (air and helium), and the result obtained in this study revealed the same as Wu et al. (28), who reported that the fountain height decreases as the temperature of the fluidizing gas increases, which is reflected in a reduction of the drag force. This study revealed that the static bed height, particle density, and the gas flow rate are the most important interacting factors that have a major effect to the fountain height, which is in agreement with the empirical correlation of Grace and Mathur (25).

As noted above, this was a preliminary part of a larger investigation involving additional spouted bed parametric variations. Thus all of the above conclusions and observations need to be considered as provisional until the additional experiments are completed.

ACKNOWLEDGEMENTS

The author wishes to express her sincere appreciation to her present and former advisors at the University of Tennessee, Prof. Robert M. Counce and Prof. Duane D. Bruns, and her graduate committee members, Prof. Ke Nguyen, Prof. Tsewei Wang, Dr. C. Stuart Daw, and Dr. Charles E.A. Finney for their continuing assistance in this research. Special thanks go to Prof. Bamin Khomami for his support.

NOMENCLATURE

Ar	Archimedes number $Ar = \frac{d_p^3 \rho_g (\rho_p - \rho_g) g}{\mu_g^2}$
d_p	Particle diameter
D_c	Bed cylinder diameter
DPSD	Dimensionless particle size distribution
e_{ss}	Particle-particle coefficient of restitution
H_0	Static particle bed height
H_f	Fountain height

Re_{ms}	Minimum spouting Reynolds number $Re_{ms} = \frac{\rho_p d_p U_{ms}}{\mu_g}$
TRISO	Tristructural-isotropic
U_{ms}	Minimum spouting velocity
U	Superficial gas velocity, based on bed cylinder

Greek Letters

ρ_s	Solids density
ρ_g	Gas density
ε_o	Loose packed voidage
ε_{mf}	Minimum fluidization voidage
ϕ_s	Particle sphericity
μ_g	Gas viscosity
ΔP_s	Pressure drop across the particles inside the spouted bed

REFERENCES

1. Kunii, D.; Levenspiel, O. (1991) *Fluidization Engineering*, 2nd Ed.; Butterworth-Heinemann: Boston.
2. Zhao, X.-L.; Yao, Q.; Li, S.-Q. (2006). Effects of draft tubes on particle velocity profiles in spouted beds. *Chem. Eng. Tech.*, 29 (7): 875.
3. Hattori, H.; Ito, S.; Onezawa, T.; Yamada, K.; Yanai, S. (2004) Fluid and solids flow affecting the solids circulation rate in spouted beds with a draft tube. *J. Chem. Eng. Japan*, 37 (9): 1085.
4. Kutsakova, V.E. (2004) Drying of liquid and pasty products in a modified spouted bed of inert particles. *Drying Tech.*, 22 (10): 2343.
5. Abdul Salam, P.; Bhattacharya, S.C. (2006) A comparative study of charcoal gasification in two types of spouted bed reactors. *Energy*, 31 (2–3): 228.
6. Villa Briongos, J.; Guardiola, J. (2005) New methodology for scaling hydrodynamic data from a 2D-fluidized bed. *Chem. Eng. Sci.*, 60 (18): 5151.
7. Bi, H.T. (2008) A discussion on minimum spout velocity and jet penetration length. *Can. J. Chem. Eng.*, 82 (1): 4.
8. San José, M.J.; Olazar, M.; Aguado, R.; Bilbao, J. (1996) Influence of the conical section geometry on the hydrodynamics of shallow spouted beds. *Chem. Eng. J.*, 62 (2): 113.
9. Glicksman, L.R. (1984) Scaling relationships for fluidized beds. *Chem. Eng. Sci.*, 39 (9): 1373.
10. Glicksman, L.R.; Hyre, M.; Woloshun, K. (1993) Simplified scaling relationships for fluidized beds. *Powd. Tech.*, 77 (2): 177.
11. Glicksman, L.R.; Hyre, M.R.; Farrell, P.A. (1994) Dynamic similarity in fluidization. *Int. J. Multiphase Flow*, 20 (1): 331.
12. Glicksman, L.R. (1988) Scaling relationships for fluidized beds. *Chem. Eng. Sci.*, 43 (6): 1419.
13. Horio, M.; Nonaka, A.; Sawa, Y.; Muchi, I. (1986) A new similarity rule for fluidized bed scale-up. *AIChE J.*, 32 (9): 1466.
14. He, Y.-L.; Lim, C.J.; Grace, J.R. (1997) Scale-up studies of spouted beds. *Chem. Eng. Sci.*, 52 (2): 329.
15. Xu, J.; Ji, Y.; Wei, W.; Bao, X.; Du, W. (2007) Scaling relationships of gas-solid spouted beds. *Fluidization XII*, RP4 (65): 537.
16. Goldschmidt, M.J.V.; Kuipers, J.A.M.; van Swaaij, W.P.M. (2001) Hydrodynamic modeling of dense gas-fluidized beds using the kinetic theory of granular flow: Effect of coefficient of restitution on bed dynamics. *Chem. Eng. Sci.*, 56 (2): 571.
17. Madonna, L.A.; Lama, R.F. (1958) The derivation of an equation for predicting minimum spouting velocity. *AIChE J.*, 4 (4): 497.
18. Mathur, K.B.; Gishler, P.E. (1955) A technique for contacting gases with coarse solid particles. *AIChE J.*, 1 (2): 157.
19. Kmiec, A. (1983) The minimum spouting velocity in conical beds. *Can. J. Chem. Eng.*, 61 (3): 274.
20. Olazar, M.; San José, M.J.; Aguayo, A.T.; Arandes, J.M.; Bilbao, J. (1993) Pressure drop in conical spouted beds. *Chem. Eng. J.*, 51 (1): 53.
21. Wang, Z.; Bi, H.T.; Lim, C.J.; Su, P. (2004) Determination of minimum spouting velocities in conical spouted beds. *Can. J. Chem. Eng.*, 82 (1): 11.
22. Fane, A.G.; Mitchell, R.A. (1984) Minimum spouting velocity of scaled-up beds. *Can. J. Chem. Eng.*, 62 (3): 437.
23. Mukhlenov, I.P.; Gorshtein, A.E. (1965). Investigation of a spouting bed. *J. Khimicheskaya Promyhslennost*, 41: 443 [cited in Ref. 24].
24. Zhou, J. (2008). Hydrodynamics and modeling of shallow spouted bed with high density particles. Ph.D. dissertation, University of Tennessee.
25. Grace, J.R., Mathur, K.B. (1978) Height and structure of the fountain above spouted beds. *Can. J. Chem. Eng.*, 56 (5): 533.
26. Day, J.-Y. (1990). Fountain height and particle circulation rate in a spouted bed. *Chem. Eng. Sci.*, 45 (9): 2987.
27. San José, M.J.; Olazar, M.; Alvarez, S.; Morales, A.; Bilbao, J. (2005) Spout and fountain geometry in conical spouted beds consisting of solids of varying density. *Ind. Eng. Chem. Res.*, 44 (1): 193.
28. Wu, S.W.; Lim, C.J.; Epstein, N. (1987). Hydrodynamics of spouted beds at elevated temperatures. *Chem. Eng. Commun.*, 62 (1): 261.